PERGAMON

Applied Thermal Engineering 22 (2002) 1969–1980

APPLIED THERMAL ENGINEERING

www.elsevier.com/locate/apthermeng

Axial effective thermal conductivities of packed beds

M. Elsari, R. Hughes *

Chemical Engineering Unit, University of Salford, Maxwell Building The Crescent, Salford M5 4WT, Manchester, UK

Received 17 May 2002; accepted 7 August 2002

Abstract

Experimental investigations have been carried out to measure axial effective thermal conductivities of packed beds for a number of particles and catalyst pellets. Measurements were made for three gases (air, nitrogen and carbon dioxide) in beds packed with ball bearings, copper chromite, chromia alumina, alumina hollow cylinders and alumina spheres. A glass vacuum vessel was employed for most measurements, but a thin wall stainless steel vessel was used in a few experiments.

Empirical correlations to predict the axial effective thermal conductivity of packed bed reactors have been derived from the experimental results.

Keywords: Axial thermal conductivities; Packed beds

1. Introduction

Packed beds are used in numerous industrial thermal systems such as chemical reactors, combustors and thermal storage units. The complex heat transfer phenomena in packed beds has been extensively analysed in the literature, mainly for its importance in the analysis and design of packed bed catalytic reactors [1,2]. In non-adiabatic reactors heat flows occur in both radial and axial directions and radial heat transfer is characterised by a radial effective thermal conductivity and a wall heat transfer coefficient.

The parameters influencing the thermal conductivity of packed beds, are the thermal conductivity of the solid phase, the thermal conductivity of the fluid phase, the fluid flow, the direction of heat flow, and the relative proportion of these phases in the bicomponent mixture. The latter is commonly described using the voidage. Bed voidage is influenced by the particle size and

* Corresponding author. Tel.: +44-161-2955081; fax: +44-161-2955380.
E-mail address: r.hughes@salford.ac.uk (R. Hughes).

1359-4311/02/$ - see front matter
PII: S1359-4311(02)00117-5

Nomenclature

d_p	particle diameter
D	reactor diameter
G	mass flow rate of fluid
k	ratio of solid and fluid thermal conductivity
k_g	gas conductivity
k_s	thermal conductivity of solid phase
k_{eax}	axial effective thermal conductivity by radiation alone
P_{eax}	axial Peclet number, $Gc_p d_p / k_{eax}$
Pr	Prandtl number, $c_p \mu / k_g$
Re	Reynolds number, Gd_p/μ
c_p	specific heat at constant pressure
t	bed temperature
t_i	inlet gas temperature
t_0	temperature at end of bed
z	axial distance in bed
Z_1, Z_2	Eqs. (3) and (4)
X_v	Eq. (3)

Greek symbols

α_w	overall heat transfer coefficient in equation (Adam)
ρ	density of fluid

shape, and the tube to particular diameter ratio, the effect of fluid flow Peclet number (P_{eax}), the turbulent diffusion parameter (K_{td}) and the fluid–solid heat transfer coefficient (h).

However, in adiabatic reactors heat flows in the axial direction and is commonly characterised by the concept of an axial effective thermal conductivity. This is particular significance in the case of non-catalytic processes such as roasting of ores where a travelling grate is employed, since these commercial beds are of large diameter with negligible radial heat losses.

Yagi et al. [3] were the first to measure the effective axial thermal conductivities of packed beds. Their axial steady state heat transfer measurements were made using adiabatic double walled glass tubes of 68 and 50 mm inside diameter. The packed bed was heated from the top by an infra-red lamp so that heat penetrated downwards into the bed, while air flowed counter currently upwards through the bed from the bottom inlet.

They found that the extent of increase of axial effective thermal conductivity with increase of flow rate was larger than that for radial conductivity, but is coincident when the Reynolds number tends to zero.

Kunii and Smith [4] published data on thermal conductivities of unconsolidated particles with flowing fluids. They found that the flow contribution in the steady state equation is not linear in Reynolds number and is affected by particle diameter. However, only a graphical presentation was given and no analytical correlation was produced.

A relation for the calculation of the values of axial effective thermal conductivities at high flow rates based on a knowledge of existing data on radial thermal conductivity, velocity profile and ratio of tube to particle diameters has been given by Bischoff [5]. In deriving the relation, it was assumed that the velocity profile is flat, that there are no radial effects, and that the effective axial thermal conductivity is constant. It was noted that the predicted values coincide with the experimental data at low flow rates and was assumed that the predicted equation could be used for high fluid flow rates.

Votruba et al. [6] have evaluated the axial effective thermal conductivity from axial temperature profiles for different particle sizes, shapes and thermal conductivities, covering a large interval of Reynolds numbers. Their experiments were carried out using a vessel with an internal diameter of 26 mm. Their results were expressed in an equation for the axial Peclet number which included the effect of significant heat transport mechanisms, but included an arbitrary constant.

The flow of gas through the void structure of beds for conditions in the range of particle Reynolds number, from 0 to 5 and temperatures of 20–650 °C has been studied by Beveridge and Haughey [7]. Their results were analysed in terms of both a continuous model and a mixing cell model. Values of the axial effective thermal conductivity to the gas thermal conductivity ratio were found to increase with Reynolds number, but eventually tended to be a constant value.

Vortmeyer and Adam [8], included the heat transfer through the walls, but in an almost adiabatic system, and proposed correlations for estimating the axial effective thermal conductivity. Their experiments were carried out using vessels with internal diameters of 86, 139, 200 and 205 mm.

Dixon et al. [9] have presented a theory for predicting of effective axial thermal conductivity from a pseudo-homogeneous model. Subsequently Dixon and Cresswell [10] departed from the assumption of the investigators listed above, that solid and fluid temperatures are equal and derived a correlation between effective axial Peclet number and the product of Reynolds number and Prandtl number.

More recently, Adnani et al. [11] have developed a model from experimental data which predicts the effective thermal conductivity of single and binary mixtures of spherical particles as a function of gas pressure. Contact areas between particles were shown to be important for larger values of the solid/gas conductivity ratio.

A number of experimental and theoretical investigations on axial thermal conductivities of packed beds have been published as given above. Whilst certain problems have been resolved by these studies, there still remains a number of areas of uncertainty in detailed analysis.

Thus, although some of the parameters can be predicted with great accuracy, there is a large dispersion of data for others, and/or the correlations are only valid in a restricted range of operating conditions. Most of the correlations have been developed for spherical particles. However, there are a number of industrial processes involving many other particle shapes.

In all cases considered the overall solid and fluid temperature profiles are considered to be identical to each other. Most investigators have used this pseudo-homogeneous model, and certainly unless there are strong interphase gradients as in some catalytic processes this approach appears justified. The present work has the aim of using the simplified approach to establish working correlations for axial effective thermal conductivities for a variety of particle shapes and varying gas conditions.

2. Experimental

Measurements of the axial effective thermal conductivity were performed using a glass reactor similar to that described in previous work in this area by Yagi et al. [3], Votruba et al. [6] and Vortmeyer and Adam [8], and a thin walled steel reactor.

The glass reactor consisted of an adiabatic cylindrical Dewar vessel consisting of a 25 mm internal diameter double walled glass tube of 0.23 m length. The annular space was evacuated between the inner and outer walls and the walls coated with silver for thermal insulation in the radial direction. Heat generation was achieved using an infra-red lamp of 375 W. The lamp was placed at the outlet of the reactor and shielded from outside of the reactor by means of sheet metal. The direction of flow of gas and heat are opposite to one another. A diagram of this reactor is shown in Fig. 1. The steel reactor was also of 25 mm internal diameter and 0.23 m length and was of 0.2 mm wall thickness. It was insulated by a layer of mineral wool to limit radial heat transfer in the bed.

Seven thermocouples of 0.5 mm diameter were used for temperature measurements in both beds. These were taken in through a hole made at the bottom of the test section near the inlet. The bed was packed from the top.

In order to simulate the conditions in a reacting gas–solid system, the bed was randomly packed with different particles which have different thermal properties. The solid particles used were as follows: ball bearings of 3.17 mm diameter stainless steel type 304; alumina hollow cylinders of 2.0 mm inside diameter, 8.0 mm outside diameter and 8.0 mm length; alumina spheres of 6.4 mm diameter, copper chromite cylinders of 3.26 diameter and 3.62 mm length and chromia alumina cylinders of 4.07 mm diameter and 4.18 mm length.

The physical properties of these particles are given in Table 1.

Air, carbon dioxide and nitrogen were supplied from cylinders. These gases passed through the rotameter and were then introduced into the bottom of the reactor so that the gas flow was counter current to the heat flow.

Usually it required 2 h to achieve a steady state condition. From the start of the experiment, temperature measurements were recorded every 15 min. When no temperature variation occurred between two successive recordings it was assumed that steady state was attained.

3. Method of calculation of the results

The calculation of axial effective thermal conductivity is based on the assumptions that the temperature of the solid and fluid are the same, that there is no radiation heat transfer, and that steady state conditions were obtained.

The heat balance for the differential height dl may be represented as the following:

$$c_pG\frac{\mathrm{d}t}{\mathrm{d}l} + k_{\mathrm{eax}}\frac{\mathrm{d}^2t}{\mathrm{d}l^2} = 0 \tag{1}$$

This equation involves the assumptions that k_{eax} and c_pG are constant in the bed. Results were calculated using two different methods i.e. the method of Yagi et al. [3] using Eq. (1) and the

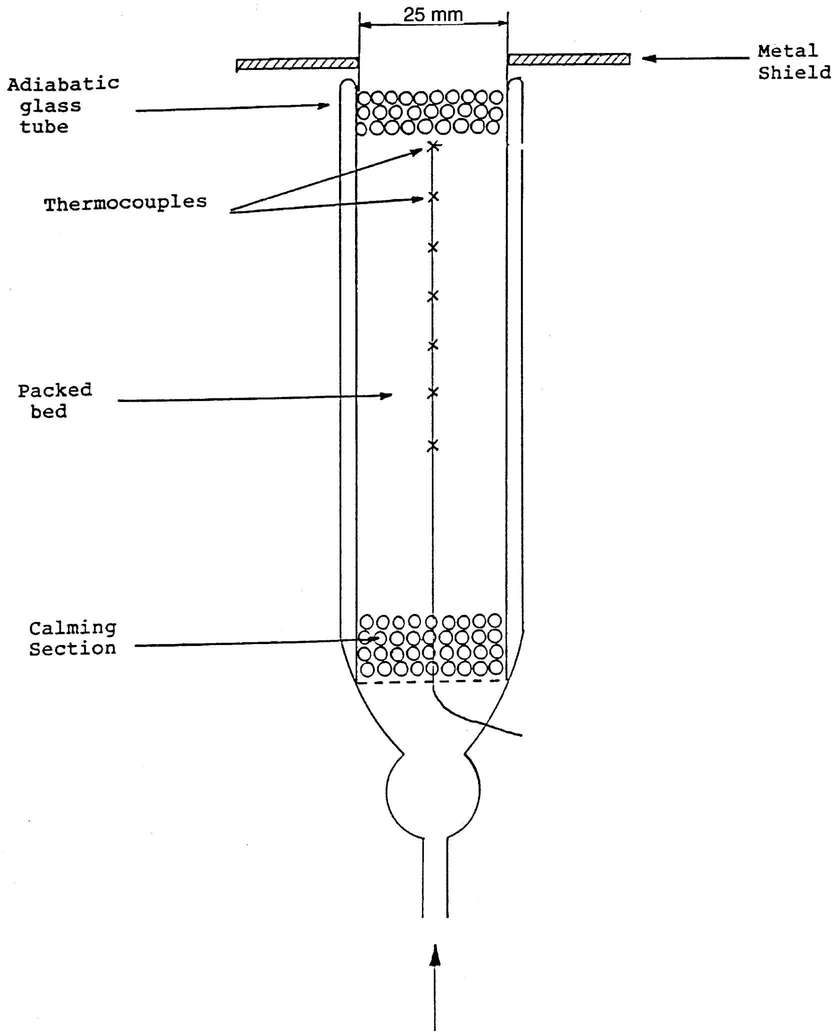

Fig. 1. Glass Dewar.

Table 1
Physical properties of particles

Particle	Diameter (mm)	Density (Kg/m^3)	Thermal conductivity (W/m k)
Ball bearings	3.17	7499	30
Alumina spheres	6.0	2816	0.68
Alumina hollow cylinders	8.0	2626	0.68
Copper chromite	3.37	2446	0.710
Chromia alumina	4.11	1712	0.65

method of Vortmeyer and Adam [9]. The latter took account of the radial heat losses by adding an overall heat loss term the pseudo-homogeneous model (Eq. (1)):

$$c_pG\frac{\mathrm{d}t}{\mathrm{d}l} + k_{\mathrm{eax}}\frac{\mathrm{d}^2t}{\mathrm{d}l^2} + \frac{4\alpha_{\mathrm{w}}}{D}(t - t_{\mathrm{i}}) = 0 \tag{2}$$

By solving the above equation the dimensionless effective thermal conductivity ($k_{\mathrm{eax}}/k_{\mathrm{g}}$) could be evaluated from Eq. (3):

$$k_{\mathrm{eax}}/k_{\mathrm{g}} = \frac{RePr}{X_{\mathrm{v}}d_{\mathrm{p}}} + \frac{Z_1^2}{X_v^2}\frac{k_{\mathrm{eax}}^{\mathrm{o}}}{k_{\mathrm{g}}} \tag{3}$$

Also Vortmeyer and Adam [8] obtained Eq. (4) for the evaluation of the stagnant conductivity.

$$\frac{k_{\mathrm{eax}}^{\mathrm{o}}}{k_{\mathrm{g}}} = \frac{1}{2d_{\mathrm{p}}Z_2}(Pr - Kd_{\mathrm{p}}Z_2) \tag{4}$$

where Z_1 and Z_2 are constants for the linear range of plots of $\ln(t - t_{\mathrm{u}})$ versus distance.

In this paper values of the stagnant conductivity ($k_{\mathrm{eax}}^{\mathrm{o}}/k_{\mathrm{g}}$) were obtained using the correlations suggested by Krupiczka [12] and Kunii and Smith [4] since the values $k_{\mathrm{eax}}^{\mathrm{o}}/k_{\mathrm{g}}$ obtained using Eq. (4) were very high ($k_{\mathrm{eax}}^{\mathrm{o}}/k_{\mathrm{g}} > 5000$ in some calculated results). Values of $k_{\mathrm{eax}}^{\mathrm{o}}/k_{\mathrm{g}}$ from correlations given by Refs. [4,12] were in broad agreement with the experimental results at $Re = 0$ (see below).

4. Results and discussion

It was necessary to ensure that the packed bed operated under adiabatic conditions. For this purpose the ball bearings were used as packing material and air was used as the gaseous medium at a flow rate of 4.65×10^{-6} m^3/s. Thermocouples were placed at the centre of the packed bed and near the wall at 9 mm from the centre. The results are shown in Table 2 and indicate that the thermocouples near the wall gave the highest reading due to wall conduction, but in no case was this greater than 4 °C and therefore the packed bed was operated at near-adiabatic conditions.

Axial effective thermal conductivities were calculated from Eq. (1) with boundary conditions

$$\begin{aligned} z &= 0 \quad t = t_0 \\ z &\to \infty \quad t = t_{\mathrm{i}} \end{aligned} \tag{5}$$

Table 2
Radial temperature variations at a flow rate of 4.65×10^{-6} m^3/s for the ball bearings/air system

Z (mm)	T (°C, $r = 0$ mm)	T (°C, $r = 9$ mm)
30	142	144
45	100	104
60	76	78
75	61	64
90	50	53
105	42	46
120	38	44

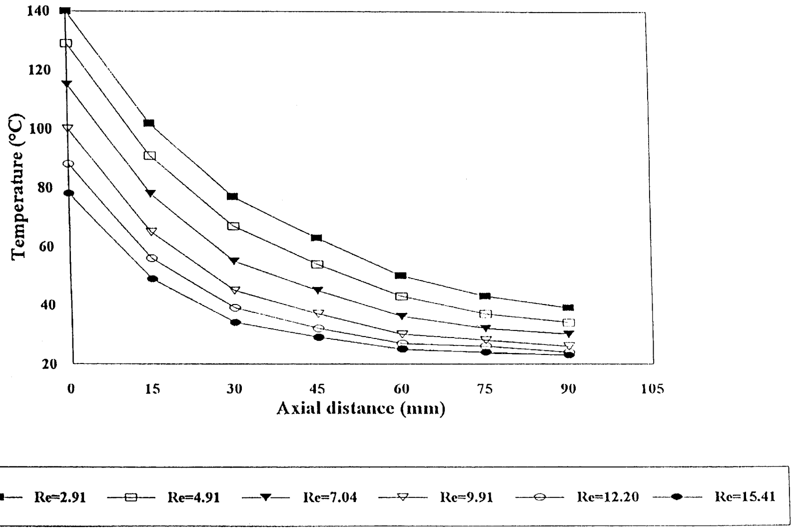

Fig. 2. Axial temperature profiles for the alumina hollow cylinders/air system using the glass Dewar.

giving in logarithmic form the equation

$$\ln(t - t_i) = \ln(t_0 - t_i) - \frac{Gc_p}{k_{eax}} z \tag{6}$$

Typical plots of temperature against length of bed are shown in Fig. 2, for the alumina hollow cylinders/air system using the glass Dewar. The corresponding logarithmic plots of $\ln(t - t_i)$ versus bed length are given in Fig. 3 from which the effective axial thermal conductivity may be calculated.

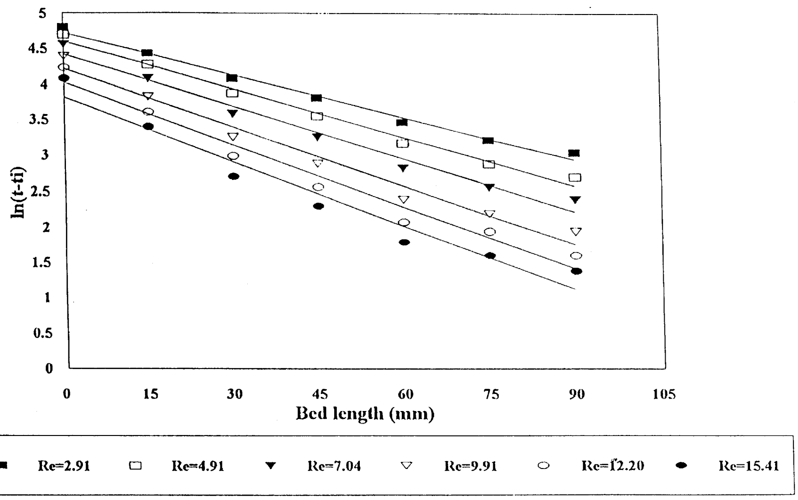

Fig. 3. Plots of $\ln(t - t_i)$ versus bed length for the alumina hollow cylinders/air system using the glass Dewar.

The experimental technique is necessarily limited to low flow rates to obtain plots such as those in Fig. 2 otherwise at higher flow rates convective processes dominate so that heat conduction against the flow is very small.

In general, from these plots it was noted that flow rates have a major effect on the maximum temperature achieved in the bed. For example, the maximum observed temperature of the bed using ball bearings as the packing material and air as the flowing gas at a volumetric flow rate of 4.65×10^{-6} m^3/s was 140 °C, while at a volumetric flow rate of 7.3×10^{-6} m^3/s the maximum temperature was 128 °C.

Also, the use of different gases influenced the maximum temperature attained in the bed. For example, at a volumetric flowrate of 7.3×10^{-6} m^3/s the maximum temperature in the bed for chromia alumina catalyst with nitrogen was 116 °C while using the same flow rate for carbon dioxide on the same catalyst, the maximum temperature was 92 °C. The reason for this is because the thermal conductivity of nitrogen is higher than that of carbon dioxide. (At 90 °C the thermal conductivity of nitrogen is 0.0297 W/m K while for carbon dioxide is 0.02034 W/m K.)

Measurements made with the stainless steel bed of 0.2 mm wall thickness showed consistently higher temperatures along the bed compared to the bed in the glass Dewar. Thus, although a thin wall metal was used, axial thermal conduction occurred along the stainless steel wall causing errors in the temperatures recorded; consequently all measurements reported here refer to those obtained with the glass Dewar.

Values of the axial effective thermal conductivity are expressed in dimensionless form representing the ratio of the axial effective thermal conductivity to the gas thermal conductivity (k^{o}_{eax}/k_{g}).

Figs. 4–6 show the effect of Reynolds number on the dimensionless axial effective thermal conductivity for the four solids used in this investigation using air, nitrogen and carbon dioxide as the gaseous media.

Fig. 4 shows the effect of Reynolds number on the dimensionless on the axial effective thermal conductivity for the 3.2 mm ball bearings for all three gas flows. It is clear that the gas environment has little effect on the value of the overall axial thermal conductivity even though the gas conductivities were varied by a factor of almost 2. Fig. 5 shows a similar plot for the alumina hollow cylinders which shows a lower effective axial thermal conductivity for a given Reynolds number compared with the ball bearings packed bed. A plot of all the results as a function of Reynolds number is given in Fig. 6 where it can be seen that the results fall into two groups. The ball bearings, copper chromite catalyst and chromia alumina catalyst can be grouped together and demonstrate higher values of the thermal conductivity compared to the alumina spheres and alumina hollow cylinders. However, the ball bearing results give slightly higher values of k_{eax}/k_{g} suggesting that there is some influence of the solid conductivity of the material. The comparable values of the metal spheres with the alumina based catalysts are explainable in terms of the similar contact areas in a packed bed, a result which was first pointed out by Masamune and Smith [13] when comparing silver compacts with compacts of lower conductivity materials.

The term Gc_p in Eq. (6) can be represented by $RePrk_{g}/d_{p}$ and hence Eq. (6) may be rewritten as

$$\ln\left(\frac{t-t_{i}}{t_{0}-t_{i}}\right) = -\left(\frac{RePrk_{g}}{d_{p}}\right)z \tag{7}$$

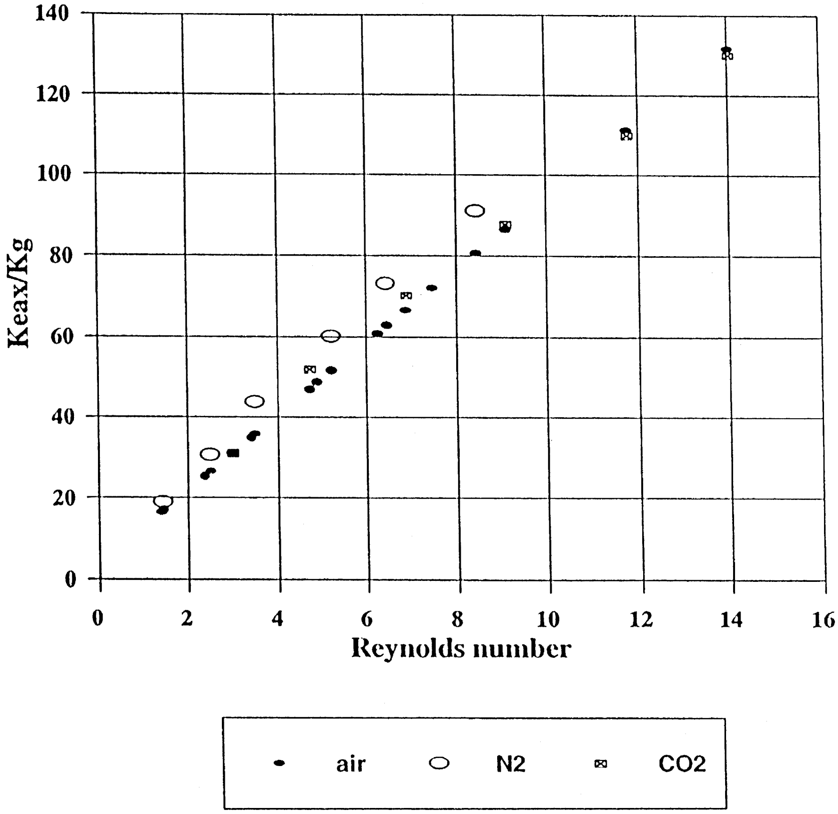

Fig. 4. Dependence of dimensionless effective axial thermal conductivity on Reynolds number for the ball bearings.

and

$$\ln\left(\frac{t - t_{\mathrm{i}}}{t_0 - t_{\mathrm{i}}}\right) = -\left(\frac{RePr}{d_{\mathrm{p}}k_{\mathrm{eax}}/k_{\mathrm{g}}}\right)z \tag{8}$$

If the data in Fig. 6 are normalised by multiplying by the individual d_{p} values then the two sets of results fall onto one line when $k_{\mathrm{eax}}/k_{\mathrm{g}}$ is plotted against Reynolds number. Hence, the original difference was due largely to the different particle sizes, although particle shape can be important, since the values of the thermal conductivity were slightly lower for the alumina hollow cylinders compared to the alumina spheres. A similar lower value was observed for Raschig rings by Yagi et al. [3].

To determine if the method of calculation influenced the values of the axial thermal conductivity, a comparison was made of values for the dimensionless axial thermal conductivity using the conventional method of Eq. (6) with the method of Vortmeyer and Adam [8]. The results are shown in Fig. 7 and indicate that good agreement between the two methods is obtained at lower Reynolds numbers but at higher Re the Vortmeyer and Adam method leads to slightly lower values. This agreement at lower Re values confirms that the system employed in the present work operates at near-adiabatic conditions since Vortmeyer and Adam's method allows for heat losses.

Empirical correlations for the axial thermal conductivity were obtained, which depended on the particles used and are shown in Table 3. These simple expressions dependent only the particle

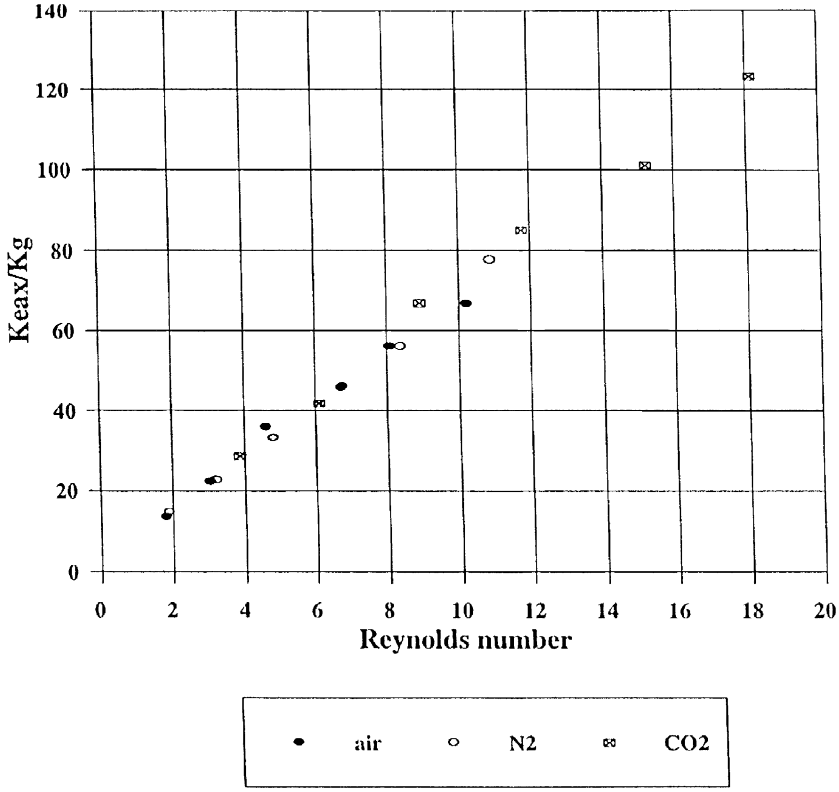

Fig. 5. Dependence of dimensionless axial thermal conductivity on Reynolds number for the alumina hollow cylinders.

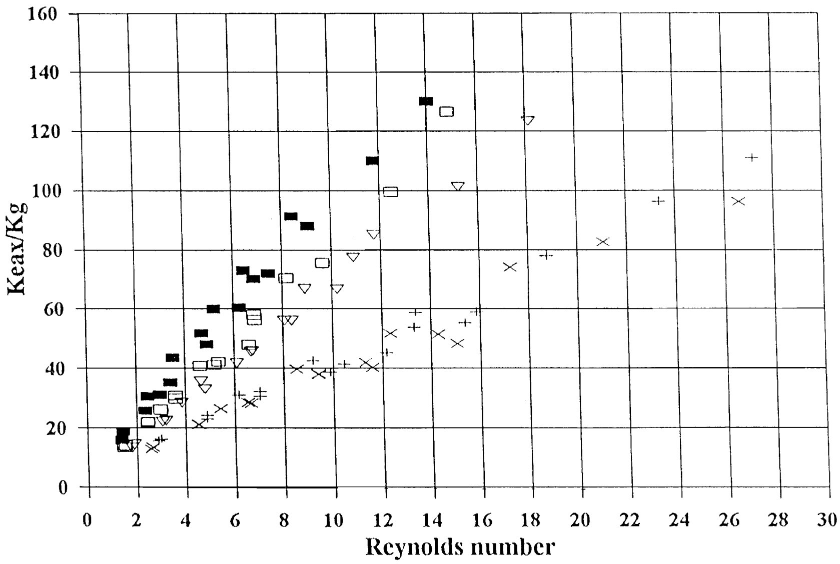

Fig. 6. Plot of k_{eax}/k_g versus Reynolds number for all particles with air as ambient gas.

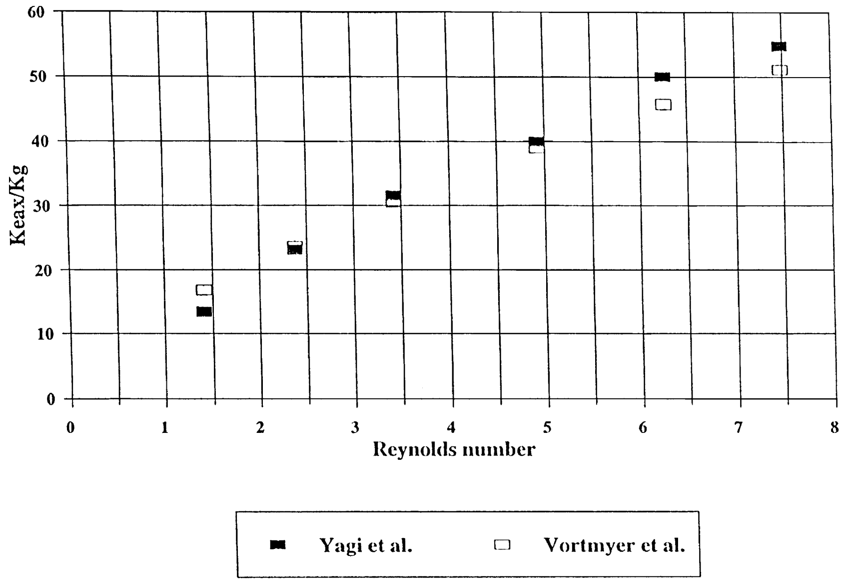

Fig. 7. Evaluation of data using two methods for the ball bearings/air system.

Table 3
Corrleations for thermal conductivity as a function or Reynolds number

Particles	Correlations
Ball bearings	$k_{eax}/k_g = 7.24 + 8.49Re$
Copper chromite	$k_{eax}/k_g = 4.25 + 7.20Re$
Chromia alumina	$k_{eax}/k_g = 3.24 + 6.47Re$
Alumina hollow	$k_{eax}/k_g = 9.68 + 3.21Re$
Alumina spheres	$k_{eax}/k_g = 8.63 + 3.12Re$

Reynolds number are justified because at the almost constant values for the Prandtl number under the present experimental conditions. Values of the coefficient on the Reynolds number showed the expected dependency on particle size, decreasing as the particle size decreased. A similar dependency has been observed in previous work. Vortmeyer and Adam quote values for this coefficient of 5 for 2 mm ball bearings in air at low Reynolds numbers, decreasing to about 3 for higher value of *Re*. For 5 mm ball bearings the corresponding values are about 2.5 and 2. Other workers have produced lower values for the coefficient varying from about 0.5 by Yagi et al. [3] and Votruba et al. [6], but there is some uncertainty regarding the treatment of results by the latter. Therefore the near agreement between the results of Vortmeyer and Adam and the present work may be considered to be reasonably satisfactory. A generalised approximate correlation for the axial effective thermal conductivity of all the materials used in the present work, can be obtained by multiplying the measured values of k_{eax}/k_g by the particle size as described above and using the k^o_{eax}/k_g values from Kapriczka [12]. This correlation may then be applied to applications of practical interest, including shallow packed beds of large diameter where the radial heat losses may now be considered insignificant in comparison with axial.

5. Conclusions

Axial effective thermal conductivities have been measured for a wide variety of catalyst particles and stainless steel ball bearings. Measurements have been made with three gas flows, namely air, nitrogen and carbon dioxide.

The results have been analysed using the conventional method using a pseudo-homogeneous model and a modified model, which accounts for heat losses. Reasonable agreement was obtained from the two methods confirming that the measurements were made under near-adiabatic conditions.

A strong dependence of axial thermal conductivity on particle size was observed, but the effect of different gases was not pronounced. Axial thermal conductivities were correlated with simple expressions involving the Reynolds number only, but, which were specific for each type of particle.

References

[1] G.F. Froment, K.B. Bischoff, Chemical Reactor Analysis and Design, J. Wiley, New York, 1979.
[2] O.M. Martinez, S.I. Pereira, I. Duarte, N.O. Lemcoff, Modelling of fixed bed catalytic reactors, Comput. Chem. Eng. 9 (1985) 535–545.
[3] S. Yagi, D. Kunii, N. Wakao, Studies on axial effective thermal conductivities in packed beds, AIChE J. 6 (1960) 543–546.
[4] D. Kunii, J.M. Smith, Heat transfer characteristics of porous rocks: II. Thermal conductivities of unconsolidated particles with flowing fluids, AIChE J. 7 (1961) 29–34.
[5] K.B. Bischoff, Axial thermal conductivities in packed beds, Can. J. Chem. Eng. 40 (1962) 161–163.
[6] J. Votruba, V. Hlavacek, M. Marek, Packed bed axial thermal conductivity, Chem. Eng. Sci. 27 (1972) 1845–1851.
[7] G.S.G. Beveridge, D.P. Haughey, Axial heat transfer in packed bed gas flow through beds between 20° and 650°, Int. J. Heat Mass Transfer 15 (1972) 953–968.
[8] D. Vortmeyer, W. Adam, Steady state measurements and analytical correlation of axial effective thermal conductivities in packed beds at low gas flow rates, Int. J. Heat Mass Transfer 27 (1984) 1465–1472.
[9] A.G. Dixon, D.L. Cresswell, Theoretical prediction of effective heat transfer parameters in packed beds, AIChE J. 25 (1979) 663–676.
[10] A.G. Dixon, D.L. Cresswell, Effective heat transfer parameters for transient packed-bed models, AIChE J. 32 (1986) 809–819.
[11] P. Adnani, I. Catton, A.R. Raffray, M.A. Abdou, Effective thermal conductivity of binary mixtures at high solid to gas conductivity ratios, Chem. Eng. Commun. 120 (1993) 45–58.
[12] R. Krupiczka, Analysis of thermal conductivity in granular materials, Int. Chem. Eng. 7 (1967) 122–143.
[13] S. Masamune, J.M. Smith, Thermal conductivity of catalyst pellets, J. Chem. Eng. Data 8 (1963) 54–58.